



ELSEVIER

Journal of Molecular Catalysis A: Chemical 161 (2000) 141–147



www.elsevier.com/locate/molcata

# Mechanism of carbon $sp^2$ -heteroatom bond cleavage in hydroprocessing of substituted benzenes over unsupported transition metal sulfides

Claude Moreau<sup>a,\*</sup>, Jacques Joffre<sup>a</sup>, Christian Saenz<sup>a</sup>, Julio Carlos Afonso<sup>b</sup>,  
Jean-Louis Portefaix<sup>b</sup>

<sup>a</sup> *Laboratoire de Matériaux Catalytiques et Catalyse en Chimie Organique, UMR 5618 ENSCM-CNRS, Ecole Nationale Supérieure de Chimie de Montpellier, 8 Rue de l'Ecole Normale, 34296 Montpellier Cedex 5, France*

<sup>b</sup> *Institut de Recherches sur la Catalyse, CNRS, 2 Avenue Albert Einstein, 69626 Villeurbanne Cedex, France*

Received 2 February 2000; accepted 5 June 2000

## Abstract

Hydroprocessing of substituted benzenes like aniline, phenol, diphenylsulfide and chlorobenzene was performed in a batch reactor over unsupported transition metal sulfides, namely Co, Ni, Nb, Mo, Ru, Rh, Pd and W sulfides at 280°C and 70 bar of hydrogen pressure. Under these experimental conditions, diphenylsulfide and chlorobenzene mainly react through initial hydrogenolysis of the carbon-substituent bond whereas aniline and phenol react through initial hydrogenation of the aromatic ring. Such a behavior was already reported for conventional sulfided cobalt- and nickel-molybdenum alumina supported catalysts. Nevertheless, these new results confirm the preponderant influence of mesomeric effects on the reactivity of organic models toward sulfided catalysts. In addition to the results obtained over the supported bimetallic sulfides, it was found from quantum chemical calculations that the hydrogenolysis rate constants correlate with the  $\pi$ -electron density on the carbon bearing the substituent and with the overall calculated  $\pi$ -electron transfer between the substituents and the benzene ring. It is thus assumed that hydrogenolysis of carbon  $sp^2$ -substituent bonds results from the attack, by a soft nucleophilic species like a hydride ion, on the carbon bearing the substituent. © 2000 Elsevier Science B.V. All rights reserved.

**Keywords:** Sulfided catalysts; Carbon  $sp^2$ -substituent bond cleavage; Reaction mechanisms

## 1. Introduction

In the presence of conventional supported hydro-treating catalysts, substituted benzenes undergo two

parallel initial reactions, namely hydrogenolysis of carbon  $sp^2$ -heteroatom bonds and hydrogenation of the aromatic ring, and it has been previously reported that they are suitable model compounds for evaluating the hydrogenolysis vs. hydrogenation activity of these catalysts [1]. It has been shown, in particular, that the influence of the electron-donating ability of the heteroatoms was less over a sulfided cobalt- than over a sulfided nickel-molybdenum alumina sup-

\* Corresponding author. Tel.: +33-04-67-14-43-20; fax: +33-04-67-14-43-49.

E-mail address: cmoreau@cit.enscm.fr (C. Moreau).

ported catalyst for the hydrogenolysis of carbon  $sp^2$ -heteroatom bonds [2]. A reduced participation of the heteroatom toward conjugation with the benzene ring through  $\pi$ -electron delocalization was proposed. As a consequence, this implied a larger participation of the heteroatom through  $\sigma$ -adsorption on the hydrogenolysis site.

Pertinent results were recently reported concerning the cleavage of carbon  $sp^3$ -nitrogen bonds over unsupported transition metal sulfides [3]. It was then interesting to reinvestigate hydrogenolysis of carbon  $sp^2$ -heteroatom bonds over the same kind of catalysts. Hydroprocessing of substituted benzenes like aniline, phenol, diphenylsulfide and chlorobenzene was then performed over unsupported transition metal sulfides, namely Co, Ni, Nb, Mo, Ru, Rh, Pd and W sulfides. This study was completed by quantum chemical calculations using the semi-empirical MNDO method, in order to get more information on the atoms implied in hydrogenolysis reactions, and on the nature of the hydrogen species involved (proton vs. hydride species).

## 2. Experimental

### 2.1. Catalysts preparation

The catalysts were prepared using methods chosen in order to get the most stable sulfide under reaction test conditions. These methods were operated at temperatures as low as possible to obtain surface areas large enough to allow accurate determination of catalytic performances.

Thus, the preparation of cobalt, nickel, rhodium and palladium sulfides was carried out according to the method developed by Pecoraro and Chianelli [4]. Niobium sulfide was prepared by direct reaction of the elements at 773 K in evacuated silica tubes (ceramic method). The decomposition of ammonium thiosalts was used for the preparation of molybdenum and tungsten sulfides [3]. Ruthenium sulfide was precipitated by  $H_2S$  from an aqueous solution of  $RuCl_3$ .

In order to stabilize each solid at temperature higher than that used for the reaction tests, the freshly prepared sulfides were treated for 4 h at 673

K either by a  $H_2$ -15%  $H_2S$  (Co, Ni, Nb, Mo, Rh, Pd and W sulfides) or a pure  $H_2S$  flow (Ru sulfide).

### 2.2. Catalysts characterization

All the sulfides were characterized by X-ray diffraction and elemental analysis. The XRD patterns were recorded using a SIEMENS D diffractometer (CuK $\alpha$  radiation) equipped with an automatic identification of phases according to the JCPDS index. Their surface areas were determined by the BET method (nitrogen adsorption at 77 K). The results of these characterizations are given in Table 1.

### 2.3. Hydroprocessing procedure

Experiments were carried out in a 0.3-l stirred autoclave (Autoclave Engineers Magne-Drive), working in the batch mode and equipped with a system for sampling of liquid during the course of the reaction without stopping the agitation.

The procedure was typically as follows. A 0.03-M solution of organic reactant in decane or dodecane (60 ml) was poured into the autoclave. The sulfided catalyst (0.3 g) was rapidly added to this solution under nitrogen to avoid contact with air. After it had been purged with nitrogen, the temperature was increased under nitrogen until it reached 280°C. Nitrogen was then removed and hydrogen was introduced at the required pressure (70 bar). Zero time was taken to be when the agitation began.

Table 1  
Characteristics of transition metal sulfides

Metal	S/ metal	Phase (R.X.)	Surface area ( $m^2 g^{-1}$ )
Co	0.89	$Co_9S_8$	43.6
Ni	1.02	$\beta NiS$	5
Nb	2.87	$NbS_3$	11
Mo	2.10	$MoS_2$	73
Ru	2.00	$RuS_2$	9
Rh	1.30	$Rh_2S_3$	16
			33
Pd	0.96	$PdS$	7.5
			20
W	2.25	$WS_2$	71
			9

## 2.4. Analyses

Analyses were performed on a Delsi 200 gas chromatograph equipped with a flame ionization detector using hydrogen as carrier gas. The wall-coated open tubular fused silica capillary columns used were Chrompack CP Sil 5 CB or CP Sil 19 CB, 25 m  $\times$  0.22 mm i.d. Products were identified by comparison with authentic samples and GC-MS analyses.

## 2.5. Kinetic measurements

The rate constants were deduced from the experimental plots by curve fitting and simulation using the AnaCin software [5], which allows calculation of the direct and reverse rate constants by taking into account adsorption of the different components.

## 2.6. Quantum chemical calculations

Electronic properties of the series of substituted benzenes and molecular orbital energies were computed by the semi-empirical MNDO quantum chemical method [6].

## 3. Results and discussion

In order to compare the catalytic properties of the different sulfides, it would have been better to obtain samples with comparable surface areas. Nevertheless, taking into account the wide variety of prepara-

Table 2

Intrinsic rate constants ( $\times 10^4 \text{ min}^{-1} \text{ m}^{-2}$ ) for hydrogenolysis of chlorobenzene, diphenylsulfide, aniline and phenol over transition metal sulfides at 280°C and 70 bar  $\text{H}_2$

Catalyst	Chlorobenzene	Diphenylsulfide	Aniline	Phenol
$\text{Co}_9\text{S}_8$	14	87	–	0.1
$\beta\text{NiS}$	33	244	–	–
$\text{NbS}_3$	5	49	–	–
$\text{MoS}_2$	1	16	0.2	0.3
$\text{RuS}_2$	19	130	–	–
$\text{Rh}_2\text{S}_3$	54	166	–	–
$\text{PdS}$	9	51	–	0.1
$\text{WS}_2$	1	7	0.4	0.8

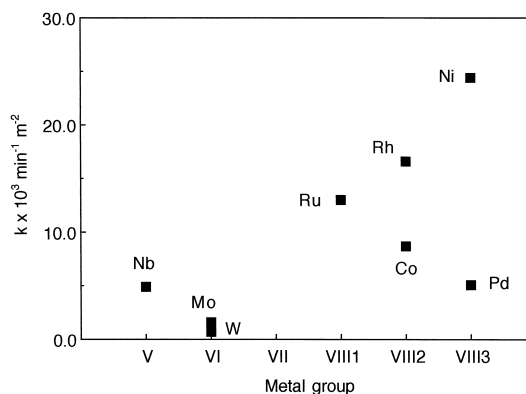


Fig. 1. Intrinsic rate constants ( $\times 10^3 \text{ min}^{-1} \text{ m}^{-2}$ ) for hydrogenolysis of diphenylsulfide over transition metal sulfides at 280°C and 70 bar  $\text{H}_2$ .

tion methods, even for a same metallic element, it was impossible to avoid variations in textural properties. It is the reason why the influence of the surface areas on the catalytic activities has been examined for different reactions where it was found that the reaction rates were nearly proportional to these surface areas. Therefore, the intrinsic rate constants (per  $\text{m}^2$ ) can be used to compare the catalytic activities of the transition metal sulfides.

### 3.1. Hydrogenolysis of the carbon $\text{sp}^2$ -substituent bonds

Table 2 reports the intrinsic rate constants for hydrogenolysis of the carbon  $\text{sp}^2$ -substituent bonds of chlorobenzene, diphenylsulfide, aniline and phenol over transition metal sulfides at 280°C and 70 bar  $\text{H}_2$ . The experimental results reported in this table show that unsupported transition metal sulfides behave like the conventional supported nickel- and cobalt-molybdenum catalysts in their sulfided state. Hydrogenolysis of the carbon  $\text{sp}^2$ -substituent bonds is the major initial reaction for slightly electron-donating substituents such as Cl and  $\text{SC}_6\text{H}_5$ . The intrinsic rate constants for hydrogenolysis of diphenylsulfide and chlorobenzene as a function of the periodic position of the metal are reported in Figs. 1 and 2, respectively.

A similar tendency is then observed for the activity of transition metal sulfides toward hydrogenolysis

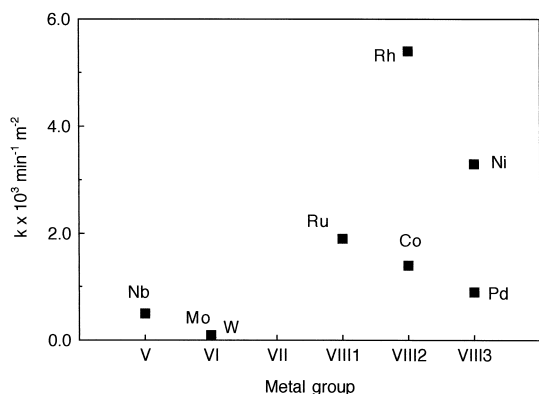


Fig. 2. Intrinsic rate constants ( $\times 10^3 \text{ min}^{-1} \text{ m}^{-2}$ ) for hydrogenolysis of chlorobenzene over transition metal sulfides at  $280^\circ\text{C}$  and  $70 \text{ bar H}_2$ .

of carbon-substituent bonds, substituents being heteroatoms or halogens. Rhodium sulfide is the most active catalyst compared to nickel sulfide for hydrogenolysis of chlorobenzene, whereas it is slightly less reactive for the cleavage of the carbon–sulfur bond of diphenylsulfide. In this latter case, the presence of  $\text{H}_2\text{S}$  as a reaction product could lead to some changes in the sulfided state of the catalyst as far as other experiments were carried out in the absence of  $\text{H}_2\text{S}$  in the feed. Another possibility would be the better affinity of Ni for negative elements such as sulfur [7].

Two other striking features deserve some comments. On one side, nickel sulfide is more active

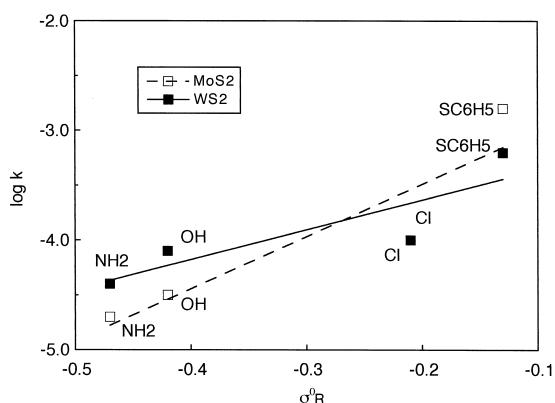


Fig. 3. Hammett plot for hydrogenolysis of the carbon  $\text{sp}^2\text{-X}$  bond in X-substituted benzenes ( $\text{X} = \text{NH}_2, \text{OH}, \text{Cl}$  and  $\text{SC}_6\text{H}_5$ ) over  $\text{MoS}_2$  and  $\text{WS}_2$  at  $280^\circ\text{C}$  and  $70 \text{ bar H}_2$ .

Table 3

Hammett  $\rho$  values for hydrogenolysis of carbon  $\text{sp}^2$ -substituent bonds over transition metal sulfides

Catalyst	$\text{Co}_9\text{S}_8$	$\text{NbS}_3$	$\text{MoS}_2$	$\text{RuS}_2$	$\text{Rh}_2\text{S}_3$	$\text{PdS}$	$\text{WS}_2$	$\text{NiS}$
$\rho$	+11	+7	+5	+15	+17	+9	+5	+11

than cobalt sulfide. This behavior was already mentioned for bimetallic sulfides where the nickel-promoted catalyst shows better hydrogenolysis properties than the corresponding cobalt-promoted catalyst [2]. On the other side, niobium sulfide, which is known for its relatively high acidic properties for hydrogenolysis of carbon  $\text{sp}^3$ -substituent bonds [3], is not as efficient for hydrogenolysis of carbon  $\text{sp}^2$ -substituent bonds. This would mean that acidity of sulfided catalysts is not as important for hydrogenolysis of such bonds than for hydrogenation reactions.

### 3.2. Hammett relationships

Hammett relationships obtained by plotting the logarithms of the rate constants as a function of the electron-donating character of the substituents are once again observed for hydrogenolysis reactions. They are similar to those observed in the case of conventional supported hydrotreating catalysts [2]. Fig. 3 illustrates this new relationship in the case of  $\text{MoS}_2$  and  $\text{WS}_2$ , where the rate constants are available for all the reactants studied. The slope  $\rho$  values calculated, or estimated as far as experimental results

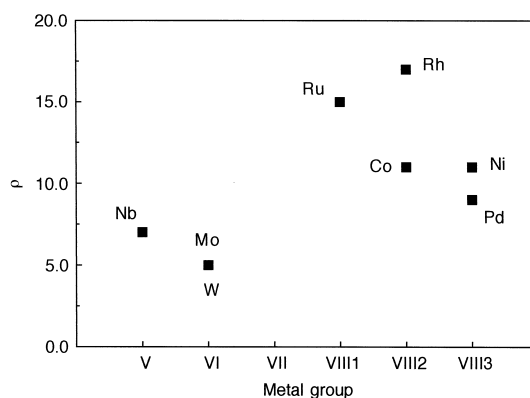


Fig. 4. Slope  $\rho$  values for hydrogenolysis of carbon-substituent bonds over transition metal sulfides.

Table 4

Overall  $\pi$ -electron transfer,  $\Sigma\Delta q_\pi$ , between the aromatic ring and the substituents,  $\pi$ -electron densities on the carbon bearing the substituent,  $C_1$ , and hydrogenolysis ( $k$ ) rate constants ( $\times 10^3 \text{ min}^{-1} \text{ g cat}^{-1}$ ) of X-substituted benzenes over sulfided NiMo and CoMo catalysts

Substituent X	$\pi$ -electron density (eV)		NiMo HR 346	CoMo HR 306
	$C_1$	$\Sigma\Delta q_\pi$	$k$	$k$
H	0	0	–	–
F	–22	–59	8	45
Cl	–61	–24	75	44
Br	–77	–21	100	60
OH	36	–93	2	28
$\text{OC}_6\text{H}_5$	15	–67	3	25
$\text{SC}_6\text{H}_5$	–87	–13	300	126
$\text{NHC}_6\text{H}_5$	19	–70	1	–
$\text{NH}_2$	24	–76	1	20

allow this estimation, for hydrogenolysis reactions, are summarized in Table 3.

For the hydrogenolysis of the C–X bond, the values of the slopes are, as expected, positive, but they differ in a large manner from one catalyst to another. By plotting the slope values as a function of the periodic position of the metal, the pattern reported in Fig. 4 is obtained. Two distinct groups of data are observed, the first one for metals from groups V and VI with low slope values, and the second group for metals from groups VIII with higher slope values. Although there is no clear explanation to account for such a phenomenon, it seems there might be some relationship with the “Hard Soft Acids and Bases” principle [8] in relation with the mechanism early proposed by Laine [9] through formation of a complex with metals from group VIII. Positive slope values imply a negatively charged transition state and an analogy with aromatic nucleophilic substitution reactions can be readily considered. Indeed, transition metal complexes are known to catalyze aromatic nucleophilic substitution reactions of halogenobenzenes [10,11]. According to the “Hard Soft Acids and Bases” Pearson principle, nucleophiles used are soft bases, particularly for the substitution of halogens by hydride ions, which are soft bases. In the presence of sulfided catalysts, the hydrogenolysis of carbon–halogen bonds follows the same reactivity pattern, thus leading to further consideration of the HSAB classification, and the presence of hydride as the active species in the hydrogenolysis step.

### 3.3. Quantum chemical determination of the active carbon center

In order to corroborate these assumptions and to get more information on the carbon atoms involved in carbon  $\text{sp}^2$ -substituent hydrogenolysis reactions, the electronic properties of the series of X-substituted benzenes have been computed by the MNDO quantum-chemical method [6]. The results concerning calculation of the overall  $\pi$ -electron transfer,  $\Sigma\Delta q_\pi$ , between the aromatic ring and the substituents, and of the  $\pi$ -electron densities on the carbon atom bearing the substituents,  $C_1$ , are reported in Table 4, together with the hydrogenolysis

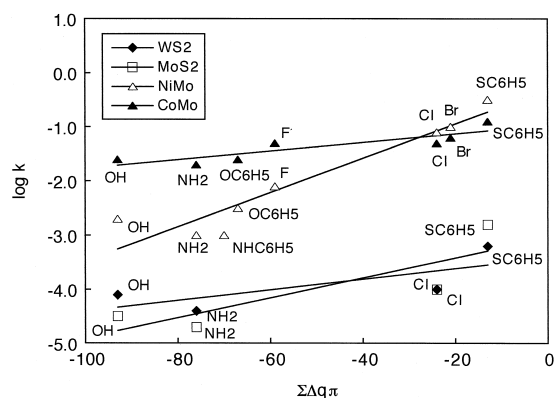


Fig. 5. Logarithms of hydrogenolysis rate constants vs. overall  $\pi$ -electron transfer over  $\text{MoS}_2$ ,  $\text{WS}_2$ , sulfided NiMo and CoMo catalysts.

rate constants obtained over sulfided NiMo and CoMo catalysts.

By plotting the logarithms of the hydrogenolysis rate constants for sulfided NiMo and CoMo catalysts as a function of these different electronic parameters, overall  $\pi$ -electron transfer,  $\Sigma\Delta q_\pi$ , between the aromatic ring and the substituents (Fig. 5) and  $\pi$ -electron densities on the carbon atom bearing the substituents,  $C_1$ , (Fig. 6) correlations of the same kind as those previously obtained as a function of the electron-donating character of the substituents are obtained. The correlation between the hydrogenolysis rate constants and the overall  $\pi$ -electron transfer  $\Sigma\Delta q_\pi$  (Fig. 5) between the aromatic ring and the substituents was expected as far as this quantum-chemical approach was already used for the calculation of Hammett coefficients [12]. Moreover, hydrogenolysis rate constants also correlate with the  $\pi$ -electron densities calculated on the carbon atom  $C_1$ . Hydrogenolysis rate constants increase with increasing the  $\pi$ -electron density on  $C_1$  atom (Fig. 6), assuming a prior oxidative addition step followed by hydride transfer, as already proposed for aromatic nucleophilic substitution reactions.

Although the number of substrates was less for the study of transition metal sulfides than for the CoMo and NiMo catalysts, a similar behavior was also obtained for hydrogenolysis over tungsten and molybdenum sulfides (Figs. 5 and 6). That confirms once again that the mechanism for hydrogenolysis of

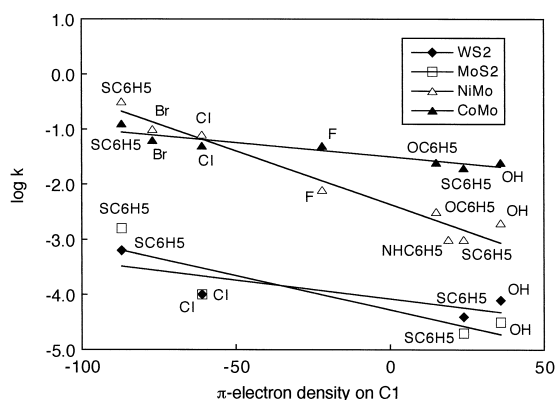


Fig. 6. Logarithms of hydrogenolysis rate constants vs.  $\pi$ -electron density on  $C_1$  over  $\text{MoS}_2$ ,  $\text{WS}_2$ , sulfided NiMo and CoMo catalysts.

Table 5

MNDO quantum chemical calculations of molecular orbital energies (eV) for X-substituted benzenes

Substituent	HOMO (eV)	LUMO (eV)
H	-9.39	0.37
F	-9.47	0.1
Cl	-9.62	-0.13
Br	-9.55	-0.09
OH	-8.88	0.25
O-C <sub>6</sub> H <sub>5</sub>	-8.87	-0.1
S-C <sub>6</sub> H <sub>5</sub>	-8.87	-0.1
NH-C <sub>6</sub> H <sub>5</sub>	-8.74	0.09
NH <sub>2</sub>	-8.77	0.31

the carbon-substituent bonds is roughly similar for both types of sulfided catalysts.

### 3.4. Quantum chemical modelling of the reactivity

The energy levels of the frontier orbitals of the reactants have been calculated using the same MNDO method [6]. The energies of the lowest unoccupied molecular orbital levels (LUMO) and the highest occupied molecular orbital levels (HOMO) are reported in Table 5.

By plotting the energies of LUMO and HOMO of the X-substituted benzenes as a function of the hydrogenolysis rate constants for both sulfided NiMo and CoMo catalysts as well as for tungsten and molybdenum sulfides, satisfactory correlations were only obtained between LUMO and the hydrogenoly-

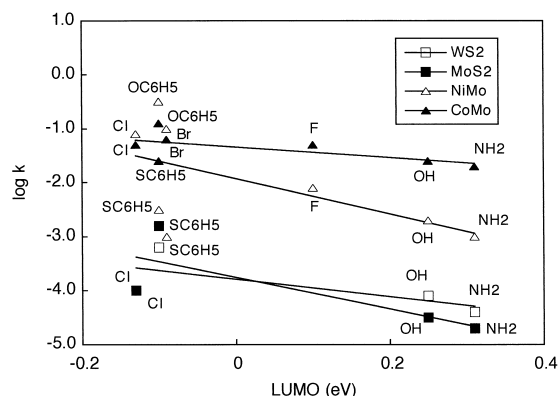


Fig. 7. Logarithms of hydrogenolysis rate constants vs. LUMO energies of substituted benzenes over  $\text{MoS}_2$ ,  $\text{WS}_2$ , sulfided NiMo and CoMo catalysts.

sis rate constants. The hydrogenolysis rate constants increase with decreasing the energy level of the lowest unoccupied orbital (Fig. 7). This corresponds to filling this anti-bonding orbital, thus weakening the  $Csp^2-X$  bond and favoring the hydrogenolysis reaction. This agrees, of course, with an attack, by a hydride species, of the carbon bearing the substituent.

#### 4. Conclusion

Experimental results obtained in the hydroprocessing of substituted benzenes over unsupported transition metal sulfides, in addition to those already obtained over supported bimetallic sulfides, lead to propose that the hydrogenolysis of carbon  $sp^2$ -substituent bonds would result from an attack, by a soft nucleophilic species like a hydride ion on the carbon bearing the substituent. Such a mechanism is fully corroborated by the presence of significant Hammett relationships and by a quantum chemical approach of the reactivity.

These conclusions are valid whatever the organic models considered in which there is a competition in

the initial stage of the reaction between saturation of aromatic rings and cleavage of  $Csp^2-X$  bonds, as, for example, in the benzofuran, benzothiophene or indole series, and dibenzofuran, dibenzothiophene or carbazole series.

#### References

- [1] C. Moreau, P. Geneste, in: J.B. Moffat (Ed.), *Theoretical Aspects of Heterogeneous Catalysis*, Van Nostrand-Reinhold, New York, 1990, p. 256.
- [2] C. Moreau, J. Joffre, C. Saenz, P. Geneste, *J. Catal.* 122 (1990) 448.
- [3] M. Cattenot, J.L. Portefaix, J. Afonso, M. Breyse, M. Lacroix, G. Pérot, *J. Catal.* 173 (1998) 366, and references therein.
- [4] T.A. Pecoraro, R.R. Chianelli, *J. Catal.* 67 (1981) 430.
- [5] J. Joffre, P. Geneste, A. Guida, G. Szabo, C. Moreau, *Modelling of Molecular Structures and Properties*, in: J.L. Rivail (Ed.), *Stud. Phys. Theor. Chem.* 71 Elsevier, Amsterdam, 1990, p. 409.
- [6] M.J.S. Dewar, W. Thiel, *J. Am. Chem. Soc.* 96 (1977) 4899.
- [7] S. Mitsui, Y. Senda, K. Konno, *Chem. Ind.* (1963) 1354.
- [8] R.G. Pearson, *J. Am. Chem. Soc.* 85 (1963) 3533.
- [9] R.M. Laine, *New J. Chem.* 11 (1987) 543.
- [10] S.T. Lin, J.A. Roth, *J. Org. Chem.* 44 (1979) 309.
- [11] E.C. Ashby, S.T. Lin, *J. Org. Chem.* 43 (1978) 1263.
- [12] A. Pross, L. Radom, *Prog. Phys. Org. Chem.* 13 (1983) 1.